Electronic Supplementary Material

Rational design of Co-S-P nanosheet arrays as bifunctional electrocatalysts for both ethanol oxidation reaction and hydrogen evolution reaction

Shuang Sheng, Ke Ye*, Linna Sha, Kai Zhu, Yinyi Gao, Jun Yan, Guiling Wang, Dianxue Cao*

Key Laboratory of Superlight Materials and Surface Technology of Ministry of Education, College of Materials Science and Chemical Engineering, Harbin Engineering University, Harbin 150001, PR China

*Corresponding authors.

E-mail addresses: yeke@hrbeu.edu.cn (K. Ye); caodianxue@hrbeu.edu.cn (D. Cao).

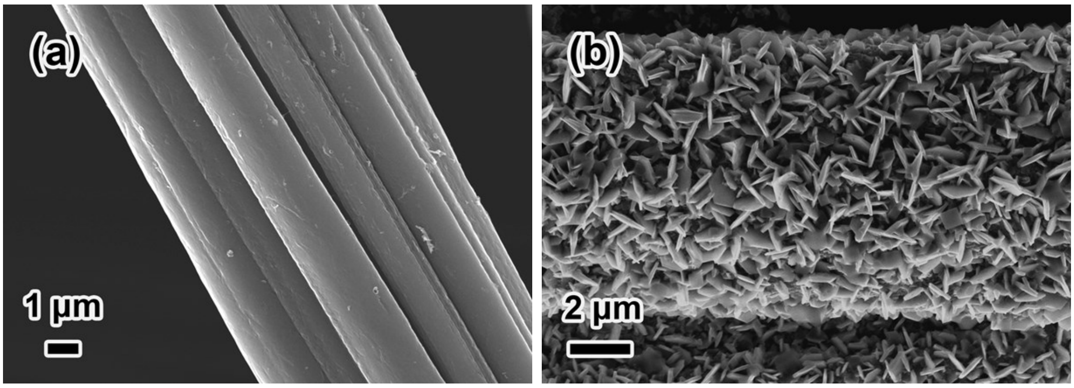

Fig. S1. SEM images of bare carbon cloth (a) and CoS_2/CC electrode (b).

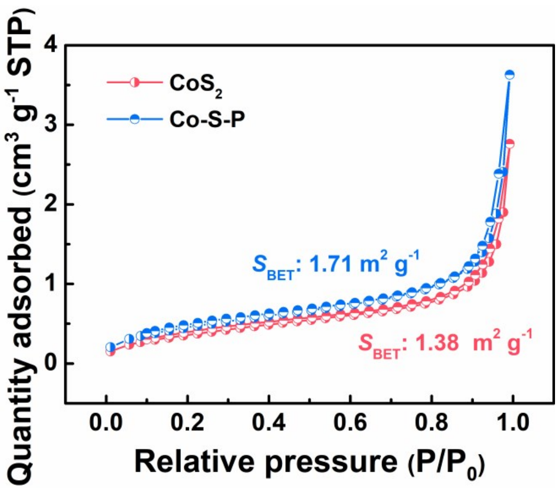

Fig. S2. Nitrogen adsorption-desorption isotherms of CoS_2 and Co-S-P.

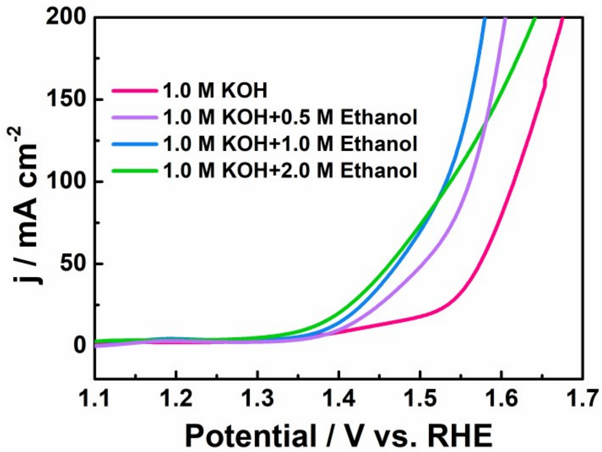

Fig. S3. LSV curves of Co-S-P/CC electrode for OER, EOR and collected using various contents of ethanol as an electrolyte.

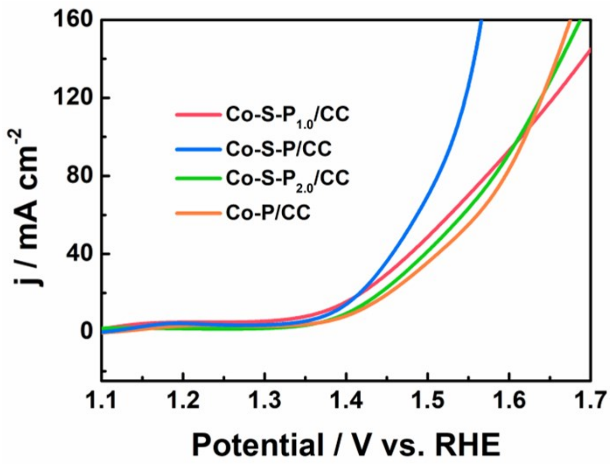

Fig. S4. LSV polarization curves of the Co-S-$P_{1.0}$/CC, Co-S-P/CC, Co-S-$P_{2.0}$ and CoP/CC toward EOR.

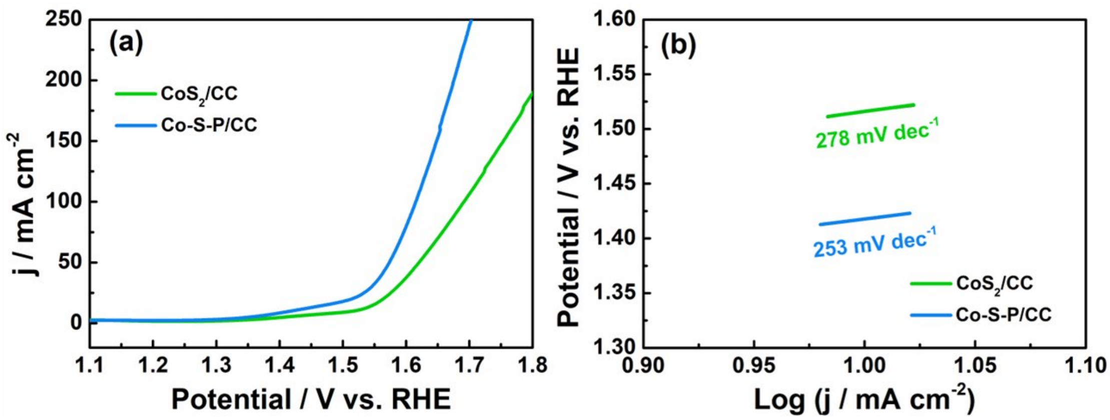

Fig. S5. (a) LSV polarization curves of the CoS_2/CC and Co-S-P/CC in 1.0 M KOH electrolyte. (b) The corresponding Tafel plots.

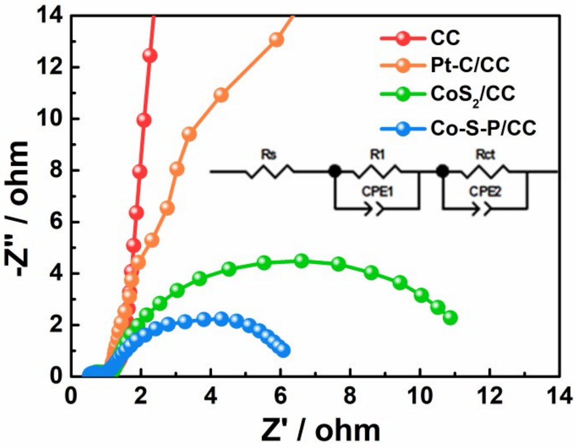

Fig. S6. Nyquist plots of the bare CC, CoS_2/CC, Co-S-P/CC catalysts for EOR process at 1.38 V vs. RHE.

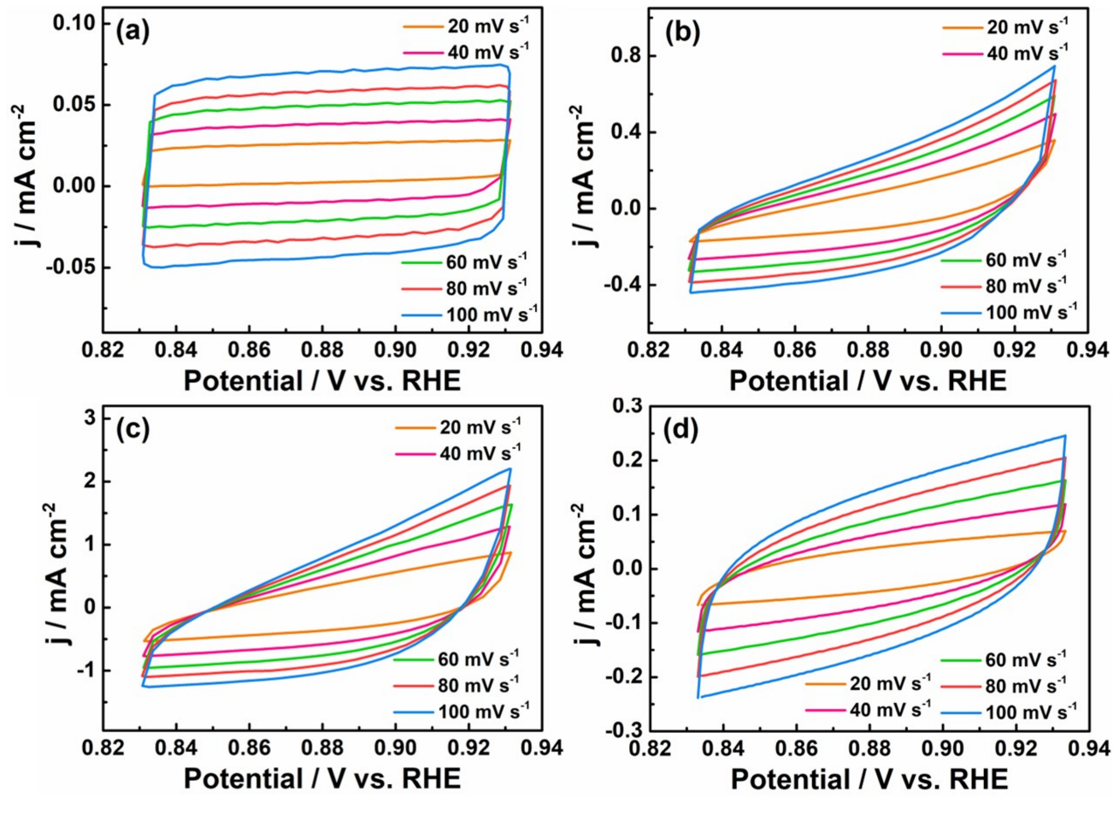

Fig. S7. CV curves for (a) bare CC, (b) CoS_2/CC, (c) Co-S-P/CC and (d) Pt-C/CC electrodes in a potential range of 0.83~0.93 V vs. RHE with scan rates from 20 to 100 mV s^{-1} upon EOR catalysis.

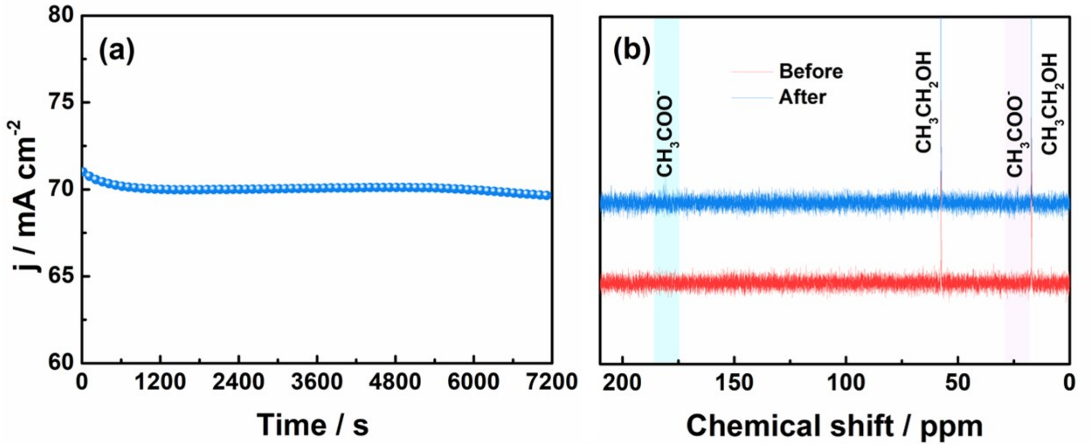

Fig. S8. (a) Chronoamperometric curves of Co-S-P/CC electrode at a potential of 1.5 V vs. RHE for 2 h. (b) ^{13}C NMR spectra of electrolyte before and after oxidation reaction.

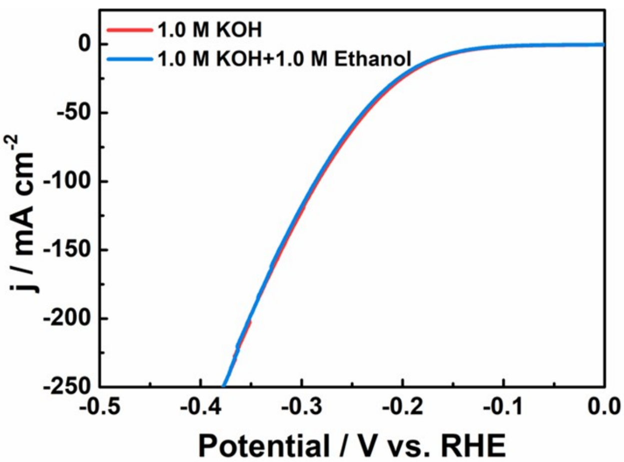

Fig. S9. LSV polarization curves of the Co-S-P/CC electrode at a scan rate of 5 mV s^{-1} in 1.0 M KOH with and without 1.0 M ethanol for HER.

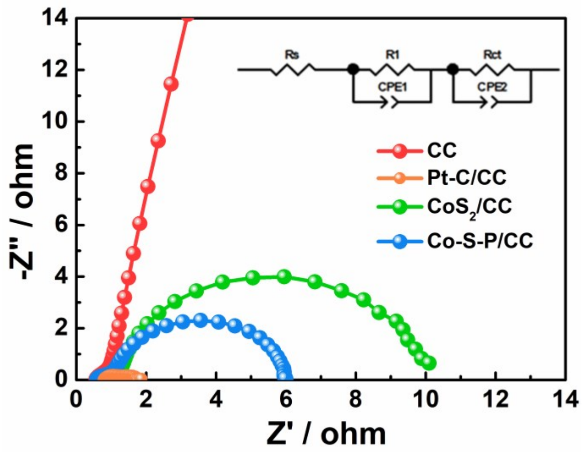

Fig. S10. Nyquist plots of the bare CC, CoS_2/CC, Co-S-P/CC catalysts at an overpotential of 200 mV toward HER.

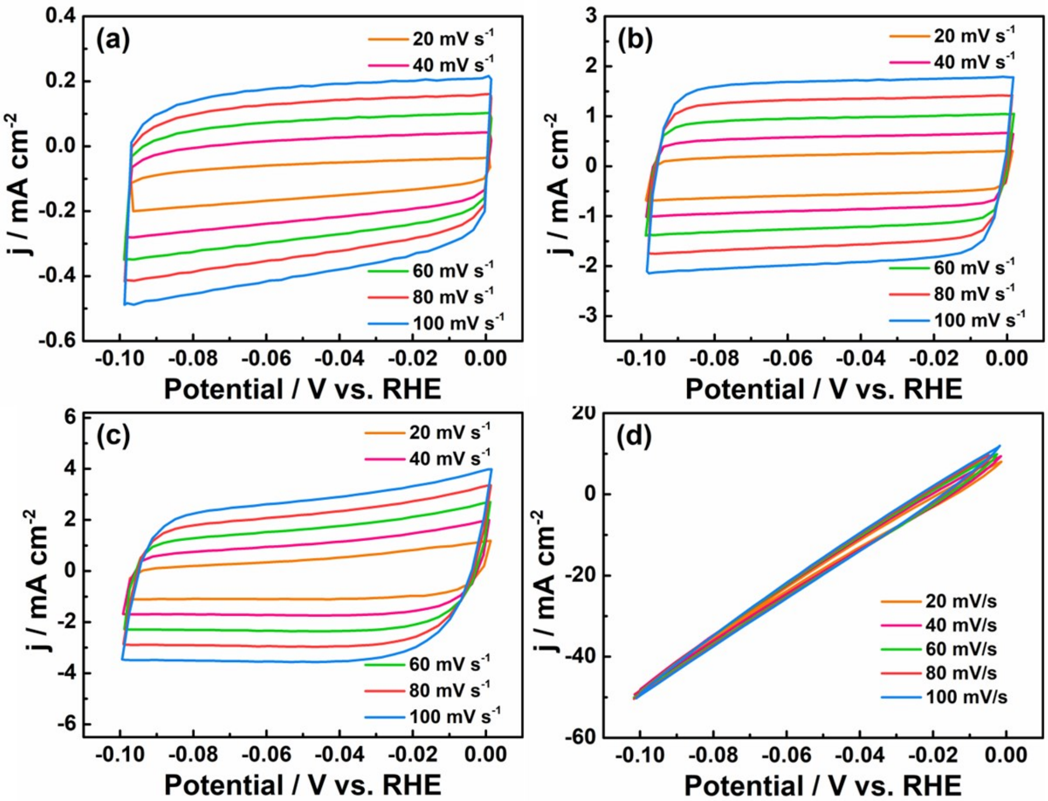

Fig. S11. CV curves for (a) bare CC, (b) CoS_2/CC, (c) Co-S-P/CC and (d) Pt-C/CC electrodes in a potential range of –0.1~0 V vs. RHE with various scan rates for HER catalysis.

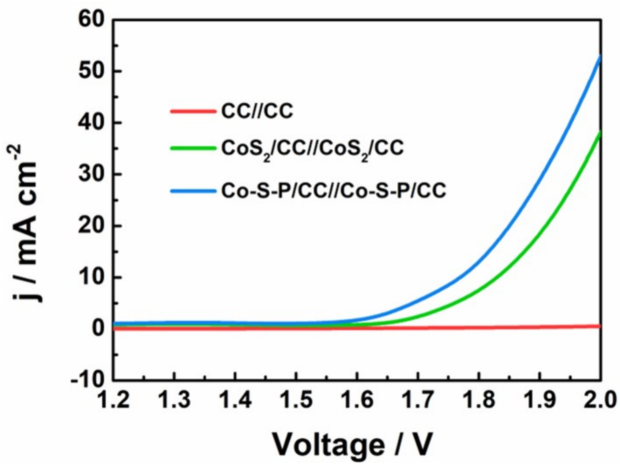

Fig. S12. Full water splitting performance of the CC, CoS_2/CC and Co-S-P/CC in a two-electrode system.

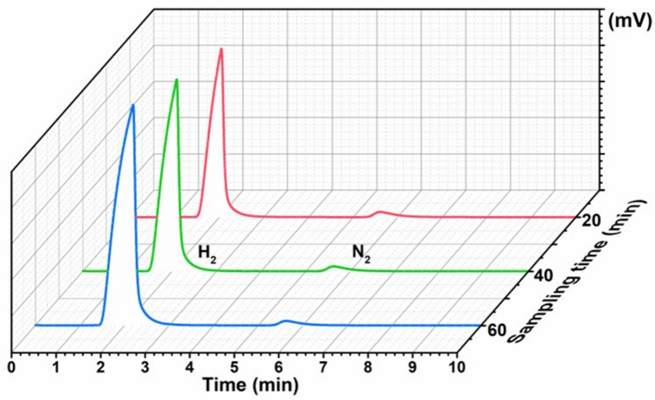

Fig. S13. Chromatograms of real-time electrolysis product of Co-S-P/CC//Co-S-P/CC electrolyser.

Table S1. Comparison with the performance of electrocatalytic ethanol oxidation catalysts reported in the previous literature

Catalysts	Electrolyte	Current density at 1.5 V vs. RHE (mA cm^{-2})	Potential at 10 mA cm^{-2} (V)	Electrolyte product	Ref.
Perforated CoNi hydroxide nanosheets	1.0 M KOH with 1.0 M ethanol	57	1.39	acetic acid	1
NGr–NiO/ITO	0.5 M NaOH with 1.0 M ethanol	3	-	-	2
MgFe layered double hydroxide	1.0 M NaOH with 1.0 M ethanol	2.2	-	-	3
NiAl layered double hydroxide	1.0 M NaOH with 1.0 M ethanol	40	1.72	Acetaldehy de acetic acid	4
NiFe layered double hydroxide	1.0 M KOH with 1.0 M ethanol	1.2	-	-	5
NiFe LDH@MnO_2 spheres	1.0 M KOH with 1.0 M ethanol	4	>1.70	-	5
Co-S-P/CC	1.0 M KOH with 1.0 M ethanol	70	1.38	acetic acid	This work

Table S2. Comparison with the performance of electrocatalytic HER catalysts reported in the previous literature

Catalysts	Electrolyte	Overpotential at 10 mA cm^{-2}	Tafel slope (mV dec^{-1})	Ref.
PdCu Alloy Nanosheets	1.0 M KOH	106 mV	124	6
PdCu Alloy Nanoparticles	1.0 M KOH	182 mV	170	6
Ni_3S_2	1.0 M KOH	335 mV	97	7
$CoNi_2S_4$@CoS_2/NF	1.0 M KOH	173 mV	51	8
$CoNi_2O_4$@Co_3O_4/NF	1.0 M KOH	206 mV	92	8
NiS_2/CFC	1.0 M KOH	210 mV	114	9
Carbon Paper/Carbon Tubes/C-S Sheets	1.0 M KOH	190 mV	131	10
Co-S-P/CC	1.0 M KOH with 1.0 M ethanol	167 mV	86	This work

Reference

1. W. Wang, Y. B. Zhu, Q. Wen, Y. Wang, J. Xia, C. Li, M. W. Chen, Y. Liu, H. Li, H. A. Wu and T. Zhai, Modulation of molecular spatial distribution and chemisorption with perforated nanosheets for ethanol electro-oxidation, *Adv. Mater.*, 2019, **31**, 1900528.
2. A. A. Daryakenari, D. Hosseini, Y. L. Ho, T. Saito, A. Apostoluk, C. R. Müller and J. J. Delaunay, Single-step electrophoretic deposition of non-noble metal catalyst layer with low onset voltage for ethanol electro-oxidation, *ACS Appl. Mater. Interfaces*, 2016, **8**, 15975-15984.
3. M. Shao, F. Ning, J. Zhao, M. Wei, D. G. Evans and X. Duan, Hierarchical layered double hydroxide microspheres with largely enhanced performance for ethanol electrooxidation, *Adv. Funct. Mater.*, 2013, **23**, 3513-3518.
4. L. Xu, Z. Wang, X. Chen, Z. Qu, F. Li and W. Yang, Ultrathin layered double hydroxide nanosheets with Ni(III) active species obtained by exfoliation for highly efficient ethanol electrooxidation, *Electrochim. Acta*, 2018, **260**, 898-904.
5. Z. Jia, Y. Wang and T. Qi, Hierarchical Ni-Fe layered double hydroxide/MnO_2 sphere architecture as an efficient noble metal-free electrocatalyst for ethanol electro-oxidation in alkaline solution, *RSC Adv.*, 2015, **5**, 83314-83319.
6. X. Zhao, L. Dai, Q. Qin, F. Pei, C. Hu and N. Zheng, Self-supported 3D PdCu alloy nanosheets as a bifunctional catalyst for electrochemical reforming of ethanol, *Small*, 2017, **13**, 1602970
7. N. Jiang, Q. Tang, M. Sheng, B. You, D. Jiang and Y. Sun, Nickel sulfides for electrocatalytic hydrogen evolution under alkaline conditions: a case study of crystalline NiS, NiS_2, and Ni_3S_2 nanoparticles, *Catal. Sci. Technol.*, 2016, **6**, 1077-1084.
8. R. Huang, W. Chen, Y. Zhang, Z. Huang, H. Dai, Y. Zhou, Y. Wu and X. Lv, Well-designed cobalt-nickel sulfide microspheres with unique peapod-like structure for overall water splitting, *J. Colloid Interface Sci.*, 2019, **556**, 401-410.
9. T. Wu, X. Zhu, G. Wang, Y. Zhang, H. Zhang and H. Zhao, Vapor-phase hydrothermal growth of single crystalline NiS_2 nanostructure film on carbon fiber cloth for electrocatalytic oxidation of alcohols to ketones and simultaneous H_2 evolution, *Nano Res.*, 2017, **11**, 1004-1017.
10. J. Wang, H. X. Zhong, Z. L. Wang, F. L. Meng and X. B. Zhang, Integrated three-dimensional carbon paper/carbon tubes/cobalt-sulfide sheets as an efficient electrode for overall water wplitting, *ACS Nano*, 2016, **10**, 2342-2348.